Journal of Environmental Quality TECHNICAL REPORTS
HEAVY METALS IN THE ENVIRONMENT

Selenium Adsorption onto Iron Oxide Layers beneath Coal-Mine Overburden Spoil

Joseph J. Donovan* and Paul F. Ziemkiewicz

A field experimental study to determine the feasibility of sequestering dissolved selenium (Se) leached from coal-mine waste rock used an iron (Fe)-oxide amendment obtained from a mine-drainage treatment wetland. Thirty lysimeters (4.9 × 7.3 m), each containing 57.7 t (1.2–1.8 m thickness) of mine-run carbonaceous shale overburden, were installed at the Hobet mine in southeastern West Virginia. The fine-grained Fe-oxide was determined to be primarily metal oxides (91.5% ferric and 4.37% aluminous), with minor (<3%) SO_4 and Ca, perhaps as gypsum. The mineralogy of the Fe was goethite, although residual ferrihydrite may have been present. Various thicknesses of this amendment (0.0064, 0.057, 0.229, and 0.457 m, plus a zero-amendment control) were used, ranging from 0 to 2.2% weight percent of the spoil. The control and each treatment were replicated six times to estimate uncertainty due to compositional and hydrological variation. Infiltration of rainfall created leachate that drained to individual batch-collection tanks that were sampled 46 times at approximately 2-wk intervals from 2010 to 2012. Basal Fe-oxide layers in the three highest amendment categories removed up to 76.1% selenium (in comparison to unamended piles) from leachate by adsorption. Only lysimeters with very thin Fe-oxide layers showed no significant reduction compared with unamended piles. Reproducibility of replicates was within acceptable limits for amended and unamended lysimeters. Results indicate that in situ amendment using Fe-oxide obtained from treatment of mine water can sequester Se by adsorption on surfaces of goethite and possibly also ferrihydrite. This process is demonstrated to substantially reduce dissolved Se in leachate and improve compliance with regulatory discharge limits.

J. Environ. Qual. 42:1402–1411 (2013)
doi:10.2134/jeq2012.0500
Received 28 Dec. 2012.
*Corresponding author (jdonovan@wvu.edu).

Selenium (Se) fate and transport in coal overburden materials may be influenced by mining and reclamation operations (Dreher and Finkelman, 1992). Predicting Se fate and transport within coal mine materials requires an understanding of the amount, form, and redox state of Se present; the mechanism(s) of solubility; and the conditions for adsorption within the spoil (Naftz and Rice, 1989). Selenium concentrations in Appalachian coal overburden lithologies have been estimated to range from 0.84 mg kg^{-1} in sandstone to 4.10 mg kg^{-1} in organic shale, generally considered the lithology with highest Se concentrations (Vesper et al., 2008). The bulk of reactive Se occurs in the fine-grained fraction (Emerson et al., 2009) and is primarily present within sulfide minerals as substitution for sulfur. It has been reported in pyrite (Vesper et al., 2008) but also has been reported in clausthalite (PbSe) and ferroselite ($FeSe_2$) (Finkelman, 1981). Pumure et al. (2010) estimated that approximately 35% of the total Se in such strata is potentially mobile. Thus, the soluble species (selenate and selenite) of Se are obtained primarily by oxidation of sulfide and/or selenide phases.

The oxidation of selenite to selenate, the more mobile aqueous species, requires a higher oxidation potential than for sulfide dissolution (McNeal and Balistrieri, 1989). Vesper et al. (2008) observed that the ratio of selenate to selenite only gradually increased downstream of source coal mines and interpreted this to be kinetically controlled. Selenite is generally the most abundant Se species reported in power plant ash materials (Huggins et al., 2007), although Hyun et al. (2006) also found significant selenate. Zhang and Sparks (1990) observed that although both aqueous phases are amenable to adsorption on crystalline iron oxides, selenite is less rapidly adsorbed but more tightly held than selenate, inasmuch as selenite tends to form inner-sphere rather than outer-sphere adsorption complexes. However, Rietra et al. (2001) observed that both selenate and selenite formed inner-sphere complexes on goethite at pH <7. Selenite and selenate can have toxicity effects on aquatic organisms due to bioaccumulation in fish and birds (Brasher and Ogle, 1993). Selenium toxicity via bioaccumulation is complex; selenate, selenite, and organo-selenium compounds have been shown to have differing toxicities in various environmental settings (Canton, 1999). Selenate is the least toxic form on an acute basis, and elevated concentrations of dissolved sulfate can reduce the magnitude of its toxicity (Brix et al., 2001). Selenium

J.J. Donovan, Dep. of Geology and Geography, 330 Brooks Hall, West Virginia Univ., Morgantown, WV 26506; P.F. Ziemkiewicz, West Virginia Water Research Institute, West Virginia Univ., Morgantown, WV 26506. Assigned to Associate Editor Scott Young.

toxicity limits have been set for aquatic organisms (USEPA, 1987), although a reliable scientific basis for setting such limits has been elusive; efforts to establish site-specific standards based on fish tissue or bird-egg concentrations have proven marginally reliable (Brix et al., 2005).

The principal environmental control limiting dissolved Se concentrations is adsorption, which has been extensively examined in laboratory investigations. Hydrous iron (Fe)-oxide or oxyhydroxide compounds, collectively referred to as "ferrihydrite," are common neutralization products of treated metal-rich mine drainage and can sequester Se by adsorption (Balistrieri and Chao, 1987, 1990). Merrill et al. (1985) observed strong pH dependency in Se adsorption; Fe-oxide removed 95% selenite at pH 4 and 80% at pH 9. Zhang and Sparks (1990) examined reaction rates of selenate and selenite sorption on goethite (α-FeOOH), a much more crystalline Fe-oxide phase that forms from recrystallization or reprecipitation of ferrihydrite. They concluded that selenite formed an inner sphere complex, whereas selenate formed a less strongly bound but more rapidly formed outer sphere complex. Su and Suarez (2001) found both ferrihydrite and goethite to be capable absorbents. They also found that ferrihydrite showed lower adsorption capacity than goethite, although Das et al. (2013) observed the opposite for selenate adsorption on synthesized Fe-oxides. Goldberg et al. (2008) determined isotherms for Se on natural soils as would be used for trench disposal of fly ash and fitted surface-complexation constants to each soil describing its anion exchange capacity. Ziemkiewicz et al. (2011) added Fe-oxide to Se-bearing mine spoil in batch reactors and found that approximately 70% of available Se was adsorbed compared with untreated controls.

Although laboratory results provide insight into adsorption capacity and mechanisms, the salient issue to the mining and regulatory sectors is the concentration and flux of total Se that will be discharged from operating mines over time. Selenium discharge dynamics under field conditions at coal mine sites are poorly understood due to the slow rate of field weathering processes, the low concentrations of Se involved, and the relatively short time for which Se has been studied in mined areas. For example, Se was not considered a pollutant in eastern US coal mines until about 2003, when several surface mines were first required to sample and report Se discharged via their regulated water outlets. There still has not been experimental study of the range of Se concentrations that might be expected to discharge from mined spoil materials via leachate with and without addition of absorbent materials and how these concentrations might vary over time. It is, however, broadly known what lithologies are expected to display the highest concentrations of Se on leaching.

Segregation of spoil units for acid mine drainage control is an established practice in the Appalachian coal fields of the United States where strata are laterally contiguous and horizontally bedded. Carbonaceous shales adjacent to coal seams tend to contain the highest concentrations of acid-forming pyrite and Se. The segregation process generally involves ripping followed by excavation via truck transport to segregation cells, either before or after coal recovery. What is not well understood is whether or how such cells of segregated waste rock might be reclaimed to minimize their impact on ambient water quality standards for Se. In particular, segregation of Se-rich rock units opens the possibility of localized treatment directed at specific lithologies to strategically limit Se release.

Another complicating factor at field scales of leaching is the heterogeneity of the composition of spoil materials and its effect on Se leaching characteristics. Large-scale surface mining in the dissected Appalachian plateau involves multiple coal seams plus overburden and interburden sequences containing a mixture of sedimentary lithologies. However, spoil created and emplaced by surface mining generally becomes well mixed but not uniform within individual sequences. Roughly half the overburden/interburden at a surface mine is moved by cast-blasting and the other half by dragline or shovel/truck haulage. Excavated spoil is generally replaced by backfill along an advancing sloped face ranging from 10 to 50 m long. Such handling methods result in a high degree of overburden blending. Although each lithology within a sequence behaves differently regarding Se mobility, spoil units are mixed composites of overburden lithologies and may display more uniform leaching behavior. If so, the results of large-scale leaching experiments should give reproducible leachate concentrations and histories.

It is well known that the hydraulic nature of fluid-flow systems that develop in coal-mine spoil is heterogeneous due to the bimodal size distribution of spoil sediments. Double-porosity characteristics, flow-through conduit-like networks, and linear-flow characteristics have been observed and documented in such flow systems (Maher and Donovan, 1997; Hawkins, 2004). In field trials, the vagaries of different fluid flow-path networks may cause differences in leaching intensity to be observed between spoil piles. As a result of the inherent variability in spoil composition and the resulting fluid-flow systems through spoil piles, large field-scale experiments must incorporate adequate replication to verify the results of experimental trials.

The aims of this study were to provide initial estimates of Se mobility in the presence of varying amounts of absorbent materials and to test for the uniformity of spoil-pile chemistry and hydrology at field, rather than laboratory, leaching scale. The materials chosen for leaching trials are rich in carbonaceous shale, characteristically the highest in Se among overburden lithologies. This study examined Se leaching and adsorption behavior over a 2-yr period of initial exposure of fresh waste-rock spoil to infiltration and weathering. The study area is the Hobet mine, Lincoln County, West Virginia (Fig. 1). This is an area where surface mining has been practiced for about 30 yr and is ongoing.

The objectives of the study were (i) to create an experimental array of large mesoscale leaching pads (lysimeters) for freshly mined carbonaceous Se-rich shale overburden, (ii) to install replicates of fresh overburden with basal underlayers of unweathered Fe-oxide in various thicknesses, (iii) to capture a complete census of leachate passing through each lysimeter and leachate volumes to create a time series of Se concentration and leachate discharge rate for an extended period of initial overburden weathering, and (iv) to examine time-series trends in Se concentration and flux, testing for differences between amended and unamended overburden and between different mass ratios of Fe-oxide.

A key element of the experimental design was to continuously collect all of the evolved leachate for each lysimeter to avoid losing individual precipitation/recharge events between discrete sampling events. Thus, sample collection was continuous even

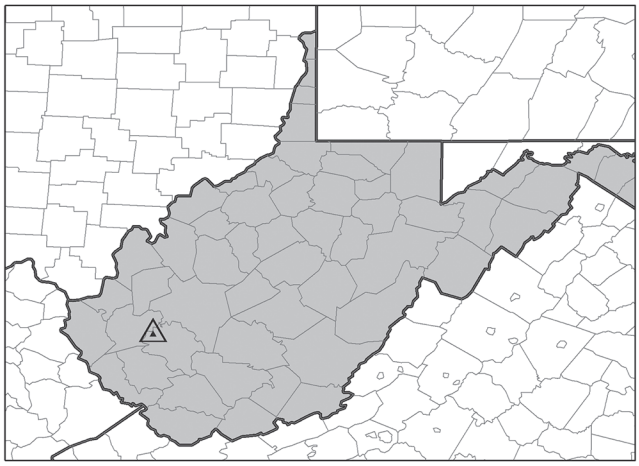

Fig. 1. Location map of the Hobet mine, Lincoln County, West Virginia.

though sampling events were discrete. Key advantages of this approach are that it allows cumulative assessment of Se and leachate flux and that no leachate is omitted from sampling due to accidents of timing. A disadvantage is that continuously collected leachate may sit for long periods between sampling events, disallowing analysis of unstable constituents (e.g., leachate oxidation-reduction potential). The Se concentration reported for each sampling date is the volume-averaged value for the antecedent period between that and the prior sampling date.

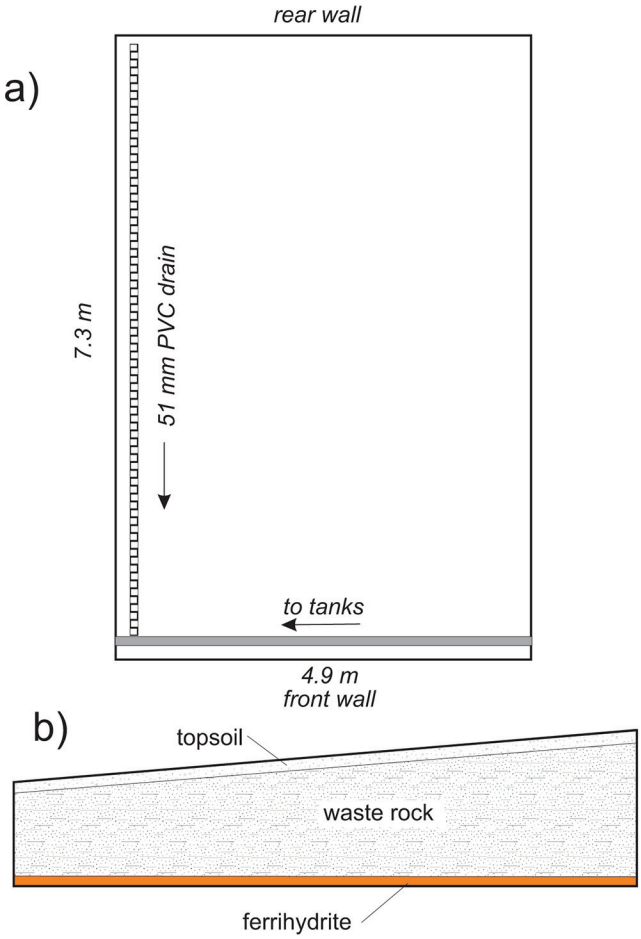

Fig. 2. (a) Plan view and (b) cross-section view of cell construction.

Materials and Methods

Experimental Array and Design

Thirty large, pan-type lysimeters of (4.9 × 7.3 m) (Fig. 2) were constructed on site at the Hobet mine in spring 2010. The individual lysimeters were constructed in a continuous array (Fig. 3) of two rows of 15 cells each separated by a 1.8-m-high plywood inner wall. The outer walls of both rows were 1.2 m high; thus, the side partitions between cells and the soil surface were sloped gently from inner to outer walls. The cells were lined along the base and sides with 0.0001-m-thick (4-mil) polyethylene and filled from bottom to top with a thin Fe-oxide layer, carbonaceous shale waste rock, and approximately 0.3 m of topsoil formed from weathered brown sandstone containing negligible soluble minerals (Fig. 2). The base of the liner was gently sloped toward a drain running the length of each lysimeter, inducing basal gravity drainage (Fig. 2). Treatments consisted of five Fe-oxide levels with six replications each. Treatments and replications were completely randomized. Each randomized experimental unit was assigned a number from 1 to 30, with a suffix to identify material composition. The slope of the lysimeter array in each row (cells 1–15 and 16–30) was about 1:20 from north to south, allowing gravity drainage of collected lysimeter leachate in that direction. Each cell contained a 2-inch, perforated-PVC lateral underdrain located along the downgradient side wall and sloped from the inner to the outer wall, where it was collected in a nonperforated, 19-mm acrylonitrile butadiene styrene pipe bundled in an array with pipes from all 15 cells in that row. These pipe bundles directed flow continuously under gravity to an array of 30 1250-L polyethylene tanks, each

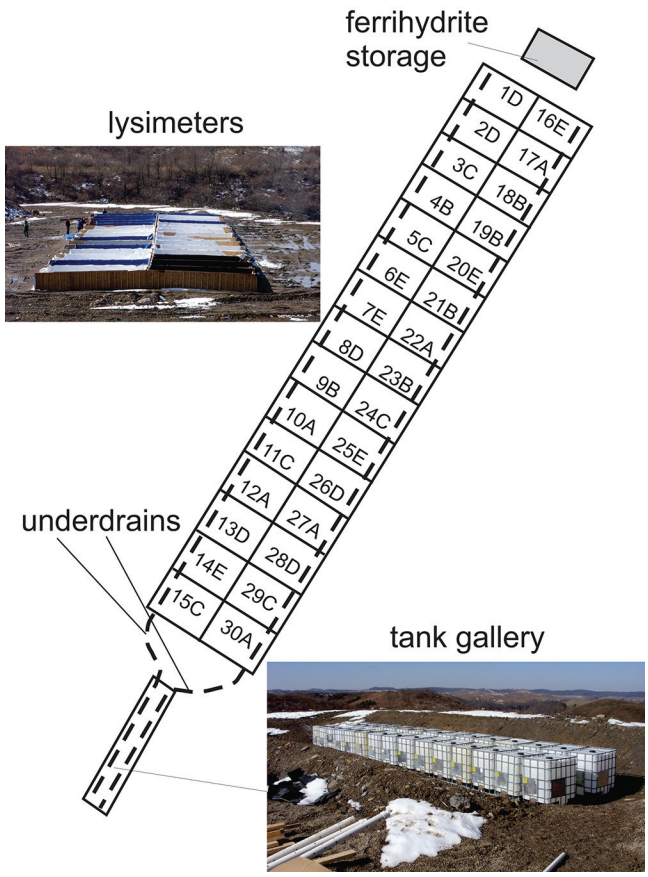

Fig. 3. Layout of lysimeter array, with labels showing ID numbers of individual cells.

receiving water from a single lysimeter (Fig. 3). Precipitation onto the soil of each cell infiltrated or ran off onto native soil around the array, allowing no runoff between or onto adjacent lysimeters. Perennial grass/legume cover on the surface of each cell induced some evapotranspiration. The difference between surface infiltration and evapotranspiration constitutes recharge into each cell. The leachate collection tank for each cell thus contained a time-integrated volume of leachate fluids collected during multiple recharge events between sampling dates.

The average depth of all materials (topsoil plus overburden plus Fe-oxide) in each cell was in the range from 1.2 to 1.8 m (Fig. 2). Shale overburden was applied in a uniform layer of thickness 0.914 ± 0.05 m (corresponding volume, 32.6 m^3). The volume of spoil in each cell was kept as uniform as possible by counting loader buckets used for each lysimeter. Using the 1.77 t m^{-3} average of Delong et al. (2012) for field estimates of mine-spoil bulk density in Appalachian Basin surface coal mines, the total mass of shaly overburden in each cell was approximately 57.7 t.

Material Composition

Each cell contained approximately the same volume of waste rock, measured by counting excavator buckets during construction, but various amounts of Fe-oxide, measured as a uniform thickness at the base of the spoil, were placed over the liner. The volume of each cell was kept uniform by varying the thickness of the surface topsoil layer to compensate for the thickness of Fe-oxide used. The waste rock was sampled during construction in three 5-gallon pails and analyzed chemically. The waste rock was freshly mined carbonaceous shale that forms the interval between the Stockton and Coalburg coal seams, Upper Kanawha Formation, Pennsylvanian age. The rock was homogeneous in appearance and was stockpiled in a single day of mining for use in this project. The Fe-oxide was obtained from a large wetland near New Stanton, Pennsylvania, in which acid mine drainage sludge had settled over a period of 30+ yr, producing a reaction product of high Fe-oxide content and uniformity. The layer thickness and weight/weight ratio of Fe-oxide to spoil for each treatment (Treatments A–E) were as follows: Treatment A, zero (0% w/w) Fe-oxide (six lysimeters); Treatment B, 0.0064 m (0.2%) Fe-oxide (six lysimeters); Treatment C, 0.057 m (1.5%) Fe-oxide (six lysimeters); Treatment D, 0.229 m (6%) Fe-oxide (six lysimeters); and Treatment E, 0.457 m (12%) Fe-oxide (six lysimeters). Therefore, the array included six identical replicates of each treatment to allow for assessment of sampling error and uncertainty in material variation and hydrologic conditions.

A sample of the Fe-oxide amendment material was analyzed for composition and mineralogy. X-ray diffraction analysis to characterize mineralogy was performed with a PANalytical Xpert Pro X-ray diffractometer with a Cu-K_α tube powered at 40 kV and 45 mA. The instrument was configured with an incident beam path antiscatter slit, a 0.04 radian Soller slits, a 0.5° divergence slit, and an Xcelerator detector. A 0.003-m-thick layer of dried sample was flush mounted in a stainless powder mount and run using a 16-s spinner stage and goniometer rotation from 5° to 75° 2θ at 0.423 min/degree. Interpretation was by search-match using the International Center for Diffraction Data PDF-2 reference phase archive. Elemental concentrations were obtained by analysis of a microwave (CEM Mars 5) digest of 0.5-g sample in 10 mL of concentrated nitric acid diluted to 50 mL. This solution was analyzed by inductively coupled plasma optical emission spectroscopy (Varian Vista Pro CCD Simultaneous ICP–OES). Values were calculated as normative oxides summing to 100%. All Fe in the sample was treated as ferric.

Water Sampling and Chemical Analysis

Sampling was performed approximately biweekly between 14 May 2010 and 1 June 2012, with 46 sampling dates for a total of 1057 water samples. On each date, the fluid volumes in the collection tanks were measured, samples were collected, and each tank was drained. Field pH, temperature, and conductivity were measured, and the filtered samples were immediately taken to the laboratory and analyzed for total Se. The water in the tanks and collection drains was found to be frozen on 10 Dec. 2010 (week 30), and sampling resumed on 8 Apr. 2011 (week 48). There were several sampling events in fall 2010 when some tanks were dry due to a lack of infiltration and no samples could be collected. Also, when tanks and lines thawed in April to May 2011, some tanks and lines took longer to re-establish flow than others. Therefore, the number of replicates for each treatment was usually, but not always, six. During exceptionally dry periods, most, if not all, replications were dry. Thus, on some dates, as few as one sample per replicate set was collected, affecting (or eliminating) estimates of precision.

Results

Characterization of Iron Oxide Amendment

Table 1 shows the chemical composition of the Fe-oxide material used as an amendment in the lysimeters presented as mass percent oxides normalized to 100%. Ferrous iron was not analyzed and was treated as negligibly small. The sludge material was 95.9% Al- and Fe-oxides (91.5% Fe-oxide). The next most concentrated elements were S (1.70% as SO_4) and Ca (0.97% as CaO). All other elements occurred in minor concentration, and Si and Se were below detection. These results are consistent with nearly pure metal oxide sludge with minor adsorbed or precipitated Ca and SO_4.

The X-ray diffraction pattern for the sample (Fig. 4) was matched to a reference phase identified as goethite (#00–008–0097 in PDF-2) that agrees with the unknown in a number of strong as well as minor peaks. The five strongest lines for this reference phase (21.09°, 33.28°, 36.81°, 41.39°, and 53.24°) were found in the unknown and are labeled in bold as "Goe" in Fig. 4. There was no clear expression in the unknown of any "6-line" ferrihydrite peaks (e.g., #00–029–712; 35.9°, 40.8°, 46.3°, 53.2°, 61.3°, 62.7°) nor of the "2 line" ferrihydrite peaks (32°, 62°) (see Das et al. [2013]); however, these lines often show considerable variation in d-spacing accompanying variable dehydration of ferrihydrite and could be masked by the goethite peaks in Fig. 4. An interpretation of the strong 26.90° peak as quartz is precluded by the nondetection of silica in the elemental data. There is a possibility that the 11.8° line is one of the two strong lines for gypsum, but the second line is overlapped by a goethite peak. There is also the possibility that a weak peak in the unknown at 18.1° is the strongest line for gibbsite (hydrous Al_2O_3). Otherwise, there are no obvious aluminum or silicate phases in the unknown, suggesting that most or all of the Al in Table 1 is in amorphous form. The X-ray diffraction may be interpreted to show that goethite dominates the crystalline

Table 1. Elemental and oxide composition of digested (0.5 g/50 mL) iron oxide amendment.

Element	Oxide	Elemental	Oxide	Oxide
		mg kg^{-1}		%
Al	Al_2O_3	201	760	4.37
Ca	CaO	121	169	0.97
Mg	MgO	35.5	58.9	0.34
Fe	Fe_2O_3	5570	15,900	91.5
Mn	MnO_2	11.1	14.3	0.08
Na	Na_2O	41.4	112	0.64
K	K_2O	28.8	69.4	0.40
Si	SiO_2	<0.1	ND†	ND
S	SO_4	98.6	296	1.70
Se	SeO_4+SeO_3	<0.6	ND	ND
			Total	100.0

† Not determined.

fraction, but there are unconfirmed minor concentrations of gibbsite, gypsum, and possibly ferrihydrite.

Time Series of Selenium Concentration

Figure 5 shows Se time series for the five treatments. Each plot shows a set of six different replicate time series for total Se concentration in one treatment class, with each replicate obtained from a different lysimeter. The Fe-oxide amendment increases from top (zero) to bottom (thickest Fe-oxide layer, 0.457 m) of the figure. This plot shows general coherence in concentration between individual replicate sets, although there was variance within treatments. In particular, the first and second replicates in all treatments (lower lysimeter ID numbers), but especially Treatments C, D, and E (the circles and triangle symbols in these plots), were notably higher than the other replicates in their sets. This could represent systematic natural variability in the refuse; all these cells were in the same portion of the array, from cells 1 through 12 (Fig. 3), and were installed consecutively. It may also be that there was some difference in the installation of these lysimeters in the composition of the refuse used for those cells, in the compaction method, or in the technique used for leveling the PVC drain line. However, overall there was relatively minor variance between replicates within treatments, and the variance was largest at times of highest Se concentration, which occurred in spring of 2010 and 2011. That is, the coefficient of variation of Se concentrations within treatments tended to be rather uniform (mean, 0.636; SD, 0.389) for low and high concentrations.

There was a gap in sampling between late November 2010 and early April 2011 caused by freezing of line drainage between the lysimeters and the tanks. During winter 2011–2012, no freezing occurred. In addition to the winter 2010–2011 data gap, several sampling events in fall 2010 and spring 2011 had fewer than six replicates per treatment because some drain lines thawed before others. Also, there were some periods in 2010 when some lysimeters produced no water during dry conditions.

Statistical Analysis of Mean Concentrations

Figure 6 shows the mean concentrations of up to six replicates within each treatment (X symbols) and the 95% confidence limits on these concentrations based on replicate standard errors and Student's t values (with $n - 1$ degrees of freedom for up to six replicates). The fitted line in all plots represents the means of Treatment A replicates (zero Fe-oxide). Some error brackets are significantly larger than others due to larger standard error

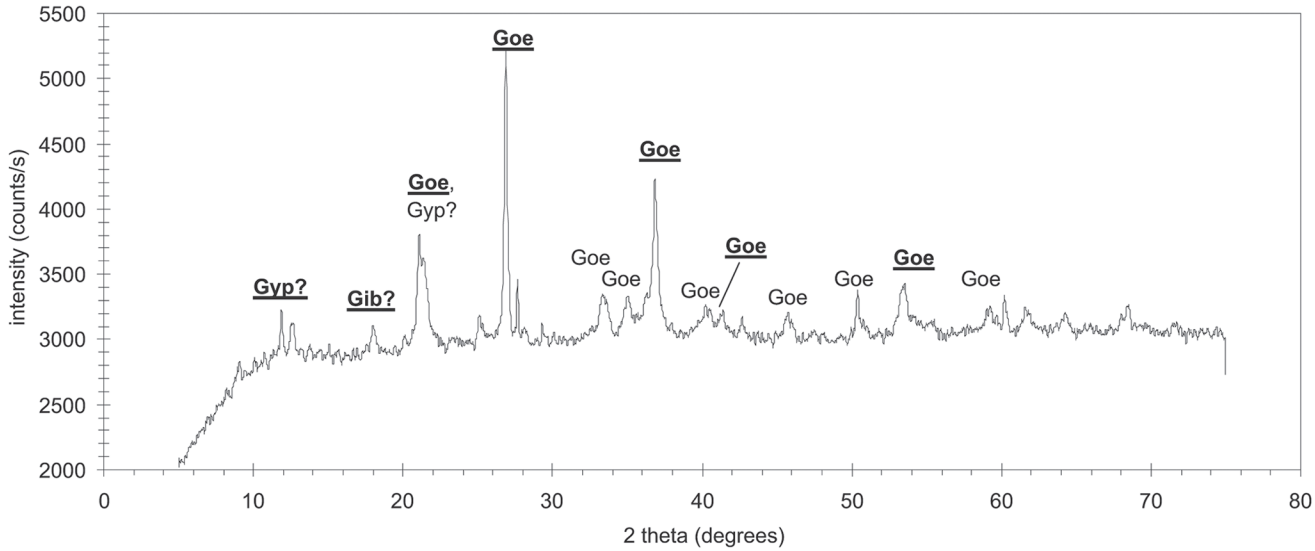

Fig. 4. X-ray diffraction pattern of Fe-oxide sediment used in lysimeters. Gib, gibbsite; Goe, goethite; Gyp, gypsum. Bold labels indicate 1 of 5 strongest lines for reference phase.

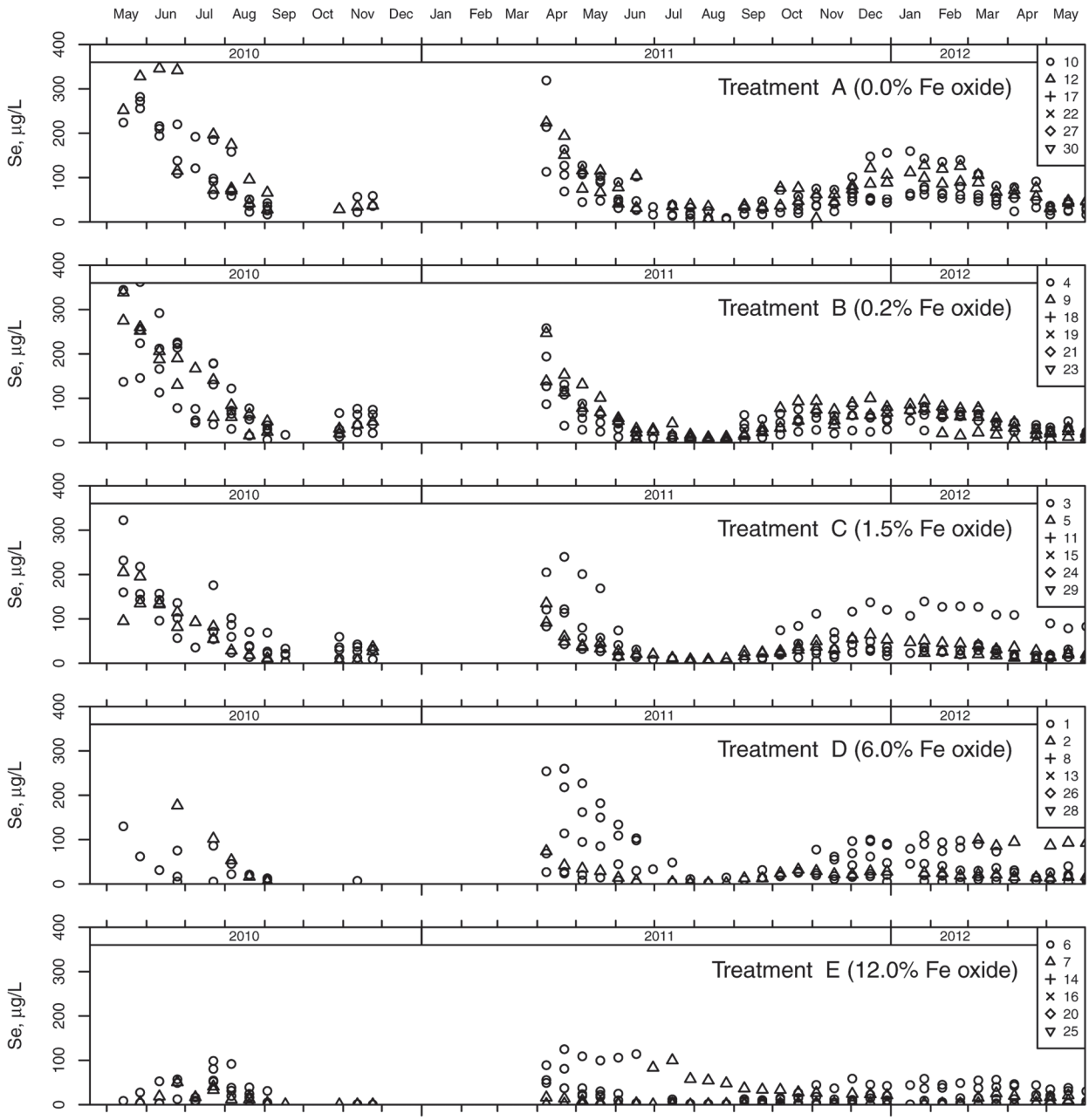

Fig. 5. Raw time series of Se concentrations arranged by treatment. Each plot shows replicates for different treatments.

within replicates for that date (usually associated with a higher mean concentration) or to fewer replicates than six due to site issues on specific dates. Treating the zero Fe-oxide mean as an unbiased estimate, the confidence range around the means of other treatments decreases from Treatment B (0.0064 m Fe-oxide) to Treatment E (0.457 m Fe-oxide). For Treatment E, there are extensive time periods when the confidence range for Se lay completely below the untreated mean Se curve. It is clear from these results that the mean Se concentrations declined in comparison to the Treatment A (control) values as the mass of Fe-oxide increased.

Selenium Fluxes

Figure 7 shows time series of Se fluxes calculated using the product of average discharge rate between sampling dates and the Se concentration averaged over the same period. The units are in g d^{-1} of total Se. There appears to be no significant difference in flux between Treatments A and B, and in fact Treatment B was higher in Se flux in the initial 3 mo of leaching and then became rather similar to Treatment A in 2011 and 2012. On the other hand, there was greater attenuation in Se loads for Treatments C, D, and E in comparison to Treatments A and B. To a higher degree than the mean concentration plots, the Se fluxes were significantly lower in the Treatment C, D, and E lysimeters than in the untreated or lightly treated lysimeters (Treatments A and B).

Figure 8 compares cumulative Se fluxes for the five treatments averaged for all replicates. Table 2 summarizes the cumulative Se flux reduction for the different amendments, and Fig. 9 summarizes the relationship between Se flux reduction and weight percent of amendment used. Treatments A and B were

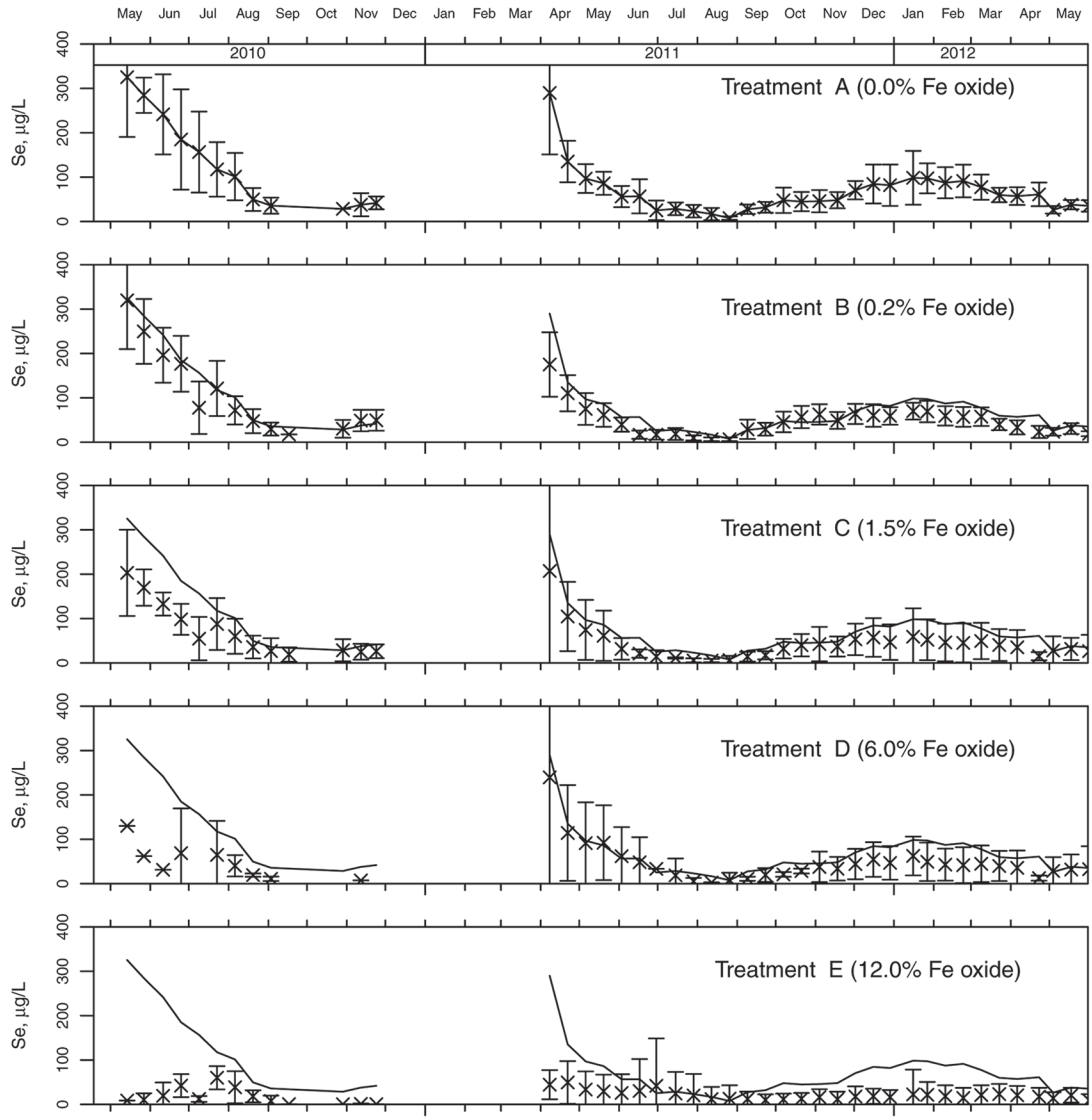

Fig. 6. Time series of mean (X symbols) and confidence intervals (95%) for Se concentrations of all replicates within treatment classes (*n* = 6 or less). The line in Treatment A is fitted to the average of its replicates. In the other plots (Treatments B–E), lines represent the same Treatment A (top plot) fit duplicated in each treatment time series.

the highest in Se loads (1.95 and 2.12 g Se, respectively) over the entire period of the experiment, with Treatment B being somewhat higher based on elevated Se concentrations in the first 3 mo. In later sampling, the A and B piles showed no significant difference in their mean fluxes. Treatment C displayed slightly lower flux than Treatment A and much less than Treatment B. Treatments D and E were substantially lower. For Treatments C, D, and E, there was an approximately linear increase in Se reduction with increasing amount of amendment used (Fig. 9). The cumulative Se flux for Treatment E at the end of the sampling period in 2012 was 76.1% lower than that of the untreated (Treatment A) lysimeters (Table 2).

Discussion

Sequestration Mechanism

These results show conclusively a large reduction in Se flux for the lysimeters using higher masses/thicknesses of Fe-oxide compared with the untreated or lightly treated cells. We attribute the reduction to adsorption of selenite and possibly selenate ion, although no redox estimates were obtained due to the batch method of sampling. There was not a proportional difference between the flux reduction of the 0.229 m (59.8% reduction) and 0.457 m (76.9% reduction) Fe-oxide layers. The use of thin Fe-oxide layers appeared to have little adsorption effect, and in fact early Se fluxes from the Treatment B piles were much higher than the controls.

Characterization of the Fe-oxide material indicates that it is primarily goethite, although it cannot be ruled out that residual ferrihydrite is present. Comparison of adsorption behavior of selenate onto synthetic ferrihydrite, goethite, and lepidocrocite was performed by Das et al. (2013). They inferred a bidentate inner-sphere surface complexation mechanism for selenate onto goethite or ferrihydrite based on Se-Fe bond distances measured by X-ray absorption spectroscopy. They also measured comparative surface areas and found ferrihydrite to be about an order of magnitude higher in surface area than goethite, leading to the expectation that goethite may require substantially higher masses than ferrihydrite for equivalent adsorption capacity. The results of this study, in which relatively large quantities of

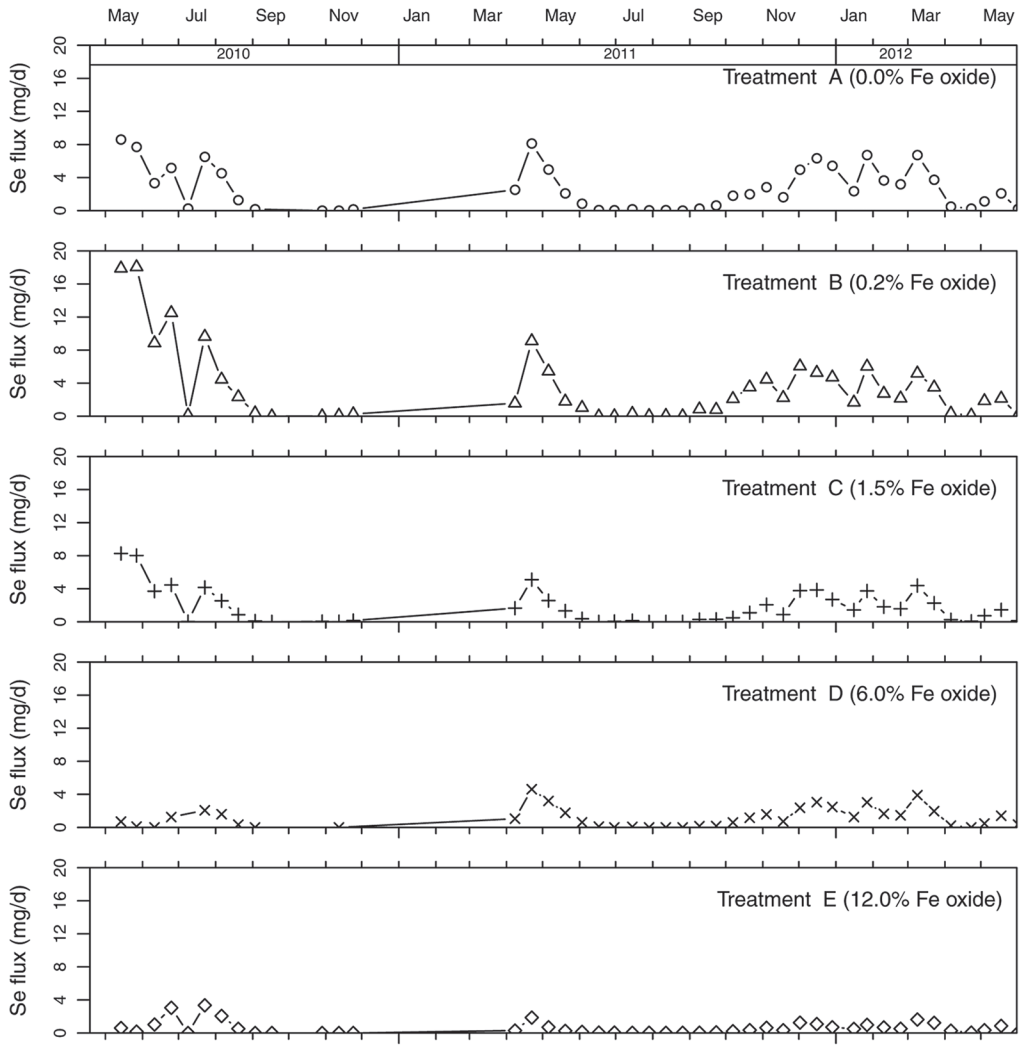

Fig. 7. Time series of mean Se flux rate (g d^{-1}) per cell for each treatment class (*n* = 6 or less).

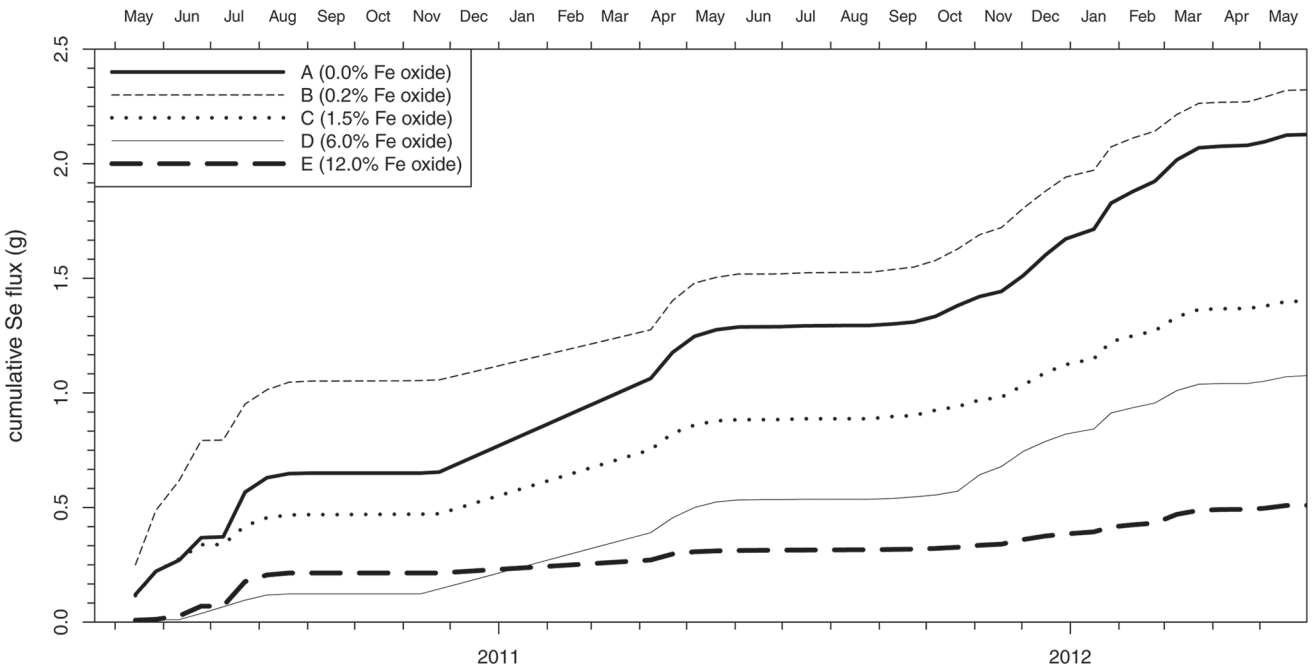

Fig. 8. Cumulative Se fluxes for the five Fe-oxide treatments.

Fe-oxide were required for sequestration of Se, are consistent with goethite being a major fraction of the Fe-oxide present.

Replication and Variability

The variability of fluxes in all treatment replicates was non-negligible but within a limited range. There were minor outliers in Se concentration in Treatments C and D. However, at most sampling events for which a full number of replicates could be sampled, the confidence intervals were reasonably low. The largest experimental errors occurred when one or more of the replicates could not be sampled due to frozen or dry conditions. In general, the replication provides convincing evidence for the reproducibility of the Se-generating potential of untreated spoil and for its sequestration by adsorption using increasing masses of Fe-oxide. This suggests that the factors of compositional variability and heterogeneous flow system behavior are, together, sufficiently low that reproducible adsorption results within treatment categories were obtained.

The most surprising outcome was the elevated flux in the Treatment B piles compared with the control. Closer examination of these data indicates that the leachate chemistry was similar between these two, but more than twice the flow was collected in the B lysimeters than the A set during the first five sampling dates of the experiment. The reason for this difference is not known because the flows were quite similar for these two sets for the duration of the experiment. Sampling error of some type in flow measurement or in sample collection for these dates is a possibility.

Selenium Mobility and Seasonality

In all treatments, strong seasonality was observed in Se concentrations and in flow rates. The "stair-step" appearance of Fig. 8 underscores the episodic nature of Se fluxes. It may be speculated that, during winter conditions, infiltration into the spoil is at minimum rate, but air ingress is continuous and encourages oxidation even while discharge of water is minimal, not only of mineral and organic fractions but also of selenite in sorbed form. The "slug" of elevated Se concentrations in spring may therefore represent flushing of over-winter reaction products. Strong Se flushes were observed in early 2010 and 2011. In 2012, the flush occurred but at lower concentration than in the first 2 yr. During drier seasons, flow and concentration of Se drop to very low levels. The seasonality of Se discharge may offer water management options for addressing periods of high concentration.

Table 2. Cumulative and average selenium flux rates versus amendment.

Treatment	Weight percent Fe-oxide	Cumulative Se flux	Reduction in Se flux	Mean Se flux rate
		g	%	g d^{-1}
A	0.0	2.12	0.0	0.00262
B	0.2	2.32	−9.4	0.00340
C	1.5	1.40	34.0	0.00174
D	6.0	1.08	49.1	0.00114
E	12.0	0.51	75.9	0.00059

Practical Implications

This sequestration trial successfully demonstrates that an inexpensive waste material (ferric iron–rich mine drainage treatment sludge) could be an effective spoil amendment to reduce and control dissolved Se outbreaks at mine scale. Organic-rich shale tends to be among the most sulfur- and selenium-rich overburden lithologies. It is often found stratigraphically above coal seams, which, in combination with its diagnostic color, makes it amenable to selective handling during the mining process. Placing layers of Fe-oxide within and at the base of selectively handled cells of organic shale may be a practical method for sequestering a significant proportion of the Se flux for an entire surface mine. Scaling these results to much larger spoil masses will require testing and optimization of the technique. Nonetheless, a simple variant of this method yielded excellent sequestration in this investigation in cells for which the mass of Fe-oxide was sufficient. Although many of the mean concentrations observed in Treatment E were higher than the 5 ppb discharge limit (maximum, 59.6 ppb; mean, 19.7 ppb), these values were 4 to 6 times lower than in unamended spoil, and after July 2011, all values remained below 20 ppb. Although monitoring continues at this site, it may be hypothesized that many of the higher concentrations occurred in the first year or so

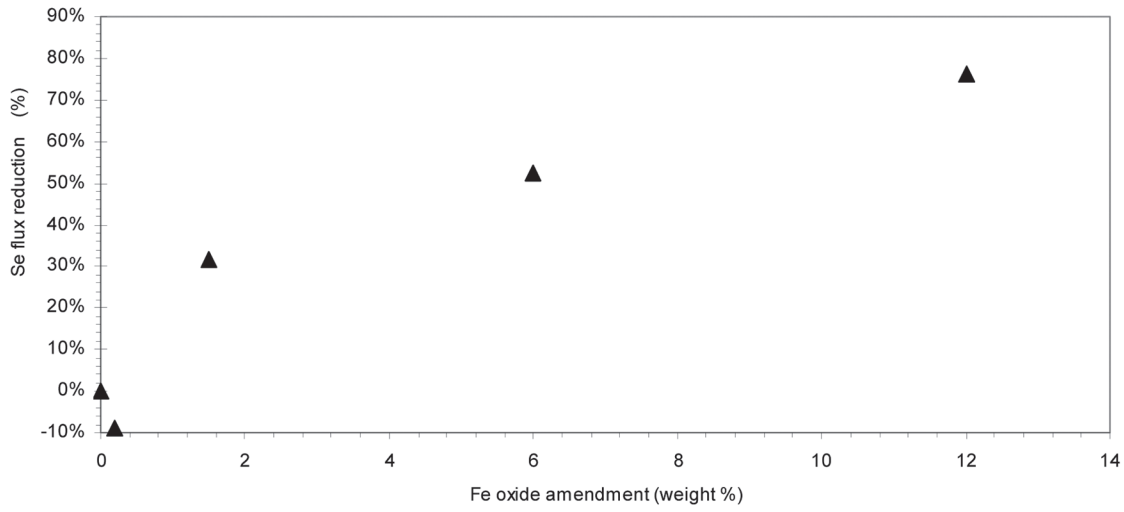

Fig. 9. Cumulative Se reduction versus Fe-oxide weight percentage in amendment.

of leaching. Given that unamended spoil generates such extreme Se concentrations in leachate, the amenability of surface mine waters to Se management without active treatment may depend on special handling techniques to control Se concentrations.

The largest Se fluxes in amended or unamended piles occurred in late winter and spring. However, during these periods, water availability from other low-Se water sources is substantial at mine sites such as these. Therefore, blending of these leachates with Se-poor water could be sufficient to meet regulatory limits on Se at points of regulated discharge.

Conclusions

This investigation was a field-scale lysimeter test of the effectiveness of a single basal Fe-oxide layer at reducing Se mobility in leachate derived from carbonaceous, shaly spoil. Key results allow the following conclusions.

Selenium concentration and flux in unamended leaching cells are by far highest during the late winter and spring months, attributed to spring flush of overwinter reaction products and to elevated recharge. Selenium fluxes are strongly seasonal, and therefore winter/spring measurements of flux are critical to long-term accurate estimation, although they are difficult to obtain. The cumulative-capture sampling method used here was useful for this purpose.

In a trial of four different layer thicknesses and mass ratios of Fe-oxide, the three thickest Fe-oxide amendments showed significant reduction in Se fluxes with respect to the control, whereas the thinnest layer showed no detectable reduction. The two thickest layers (0.229 and 0.457 m) showed a cumulative reduction in Se flux of 52 and 76%, respectively.

The six replicates within each treatment class showed that variability in experimental materials, lysimeter construction, and vadose hydrology of individual lysimeters was within acceptable limits. The results may be considered reproducible even at the large scale of the lysimeter experiments. This is especially important for the unamended piles, on the basis of which the inferred reduction in Se fluxes are calculated using results from amended piles.

The observed reductions in mean Se concentrations and fluxes are considered to have been significant and caused by an adsorption mechanism involving goethite formed from historic treatment of mine drainage in a treatment wetland. The general technique of using Fe-oxide sludges or similar waste materials as an absorbent for Se at mine sites is novel and merits study for further implementation.

Acknowledgments

This work was supported by grants from the US Office of Surface Mining Applied Science Program and the Appalachian Research Initiative for Environmental Science. The cooperation of Patriot Coal Co., which constructed the lysimeters and provided site access, was fundamental to the success of the project. Sampling assistance and selenium analysis were provided by REI Consultants, Beaver, WV. The authors thank Louis McDonald for solids digestion and Liviu Magean for inductively coupled plasma analysis of the digests.

References

Balistrieri, L.S., and T.T. Chao. 1987. Selenium adsorption by goethite. Soil Sci. Soc. Am. J. 51:1145–1151. doi:10.2136/sssaj1987.03615995005100050009x

Balistrieri, L.S., and T.T. Chao. 1990. Adsorption of selenium by amorphous iron oxyhydroxide and manganese dioxide. Geochim. Cosmochim. Acta 54:739–775. doi:10.1016/0016-7037(90)90369-V

Brasher, A.M., and R.S. Ogle. 1993. Comparative toxicity of selenite and selenate to the amphipod Hyalella azteca. Arch. Environ. Contam. Toxicol. 24:182–186. doi:10.1007/BF01141346

Brix, K.V., J.S. Volosin, W.J. Adams, R.J. Reash, R.G. Carlton, and D.O. Mcintyre. 2001. Effects of sulfate on the acute toxicity of selenate to freshwater organisms. Environ. Toxicol. Chem. 20:1037–1045. doi:10.1002/etc.5620200514

Brix, K.V., J.E. Toll, L.M. Tear, D.K. DeForest, and W.J. Adams. 2005. Setting site-specific water-quality standards by using tissue residue thresholds and bioaccumulation data. Part 2. Calculating site-specific selenium water-quality standards for protecting fish and birds. Environ. Toxicol. Chem. 24:231–237. doi:10.1897/03-471.1

Canton, S.P. 1999. Acute aquatic life criteria for selenium. Environ. Toxicol. Chem. 18:1425–1432. doi:10.1002/etc.5620180712

Das, S., M.J. Hendry, and J. Essilfie-Dughan. 2013. Adsorption of selenate onto ferrihydrite, goethite, and lepidocrocite under neutral pH conditions. Appl. Geochem. 28:185–193. doi:10.1016/j.apgeochem.2012.10.026

Delong, C., J. Skousen, and E. Pena-Yewtukhiw. 2012. Bulk density of rocky mine soils in forestry reclamation. Soil Sci. Soc. Am. J. 76:1810–1815. doi:10.2136/sssaj2011.0380n

Dreher, G.B., and R.B. Finkelman. 1992. Selenium mobilization in a surface coal mine, Powder River Basin, Wyoming, USA. Environ. Geol. Water Sci. 19:155–167. doi:10.1007/BF01704083

Emerson, P., J.G. Skousen, and P.F. Ziemkiewicz. 2009. Survival and growth of hardwoods in brown versus gray sandstone on a surface mine in West Virginia. J. Environ. Qual. 38:1821–1829. doi:10.2134/jeq2008.0479

Finkelman, R.B. 1981. Modes of occurrence of trace elements in coal. Open-File Report OFR-81–99. USGS, Weston, VA.

Goldberg, S., S. Hyun, and L.S. Lee. 2008. Chemical modeling of arsenic(III, V) and selenium(IV, VI) adsorption by soils surrounding ash disposal facilities. Vadose Zone J. 7:1231–1238. doi:10.2136/vzj2008.0013

Hawkins, J.W. 2004. Predictability of surface mine spoil hydrologic properties in the Appalachian Plateau. Ground Water 42:119–125. doi:10.1111/j.1745-6584.2004.tb02457.x

Huggins, F.E., C.L. Senior, P. Chu, K. Ladwig, and G.P. Huffman. 2007. Selenium and arsenic speciation in fly ash from full-scale coal-burning utility plants. Environ. Sci. Technol. 41:3284–3289. doi:10.1021/es062069y

Hyun, S., P.E. Burns, I. Murarka, and L.S. Lee. 2006. Selenium (IV) and (VI) sorption by solid surrounding fly ash management facilities. Vadose Zone J. 5:1110–1118. doi:10.2136/vzj2005.0140

Maher, T.P., and J.J. Donovan. 1997. Double-flow behavior observed in well tests of an extremely heterogeneous mine-spoil aquifer. Eng. Geol. 48:83–99. doi:10.1016/S0013-7952(97)81915-1

McNeal, J.M., and L.S. Balistrieri. 1989. Geochemistry and occurrence of selenium: An overview. In: L.W. Jacobs, editor, Selenium in agriculture and the environment. SSSA Spec. Pub. 23. SSSA, Madison, WI. p. 1–13.

Merrill, D.T., P.M. Maroney, and D.S. Parker. 1985. Trace element removal by coprecipitation with amorphous iron oxyhydroxide:engineering evaluation. Rep. EPRI, CS 4087. Electric Power Research Institute, Coal Combustion Systems Division, Palo Alto, CA.

Naftz, D.L., and J. Rice. 1989. Geochemical processes controlling selenium in ground water after mining, Powder River Basin, Wyoming, USA. Appl. Geochem. 4:565–576. doi:10.1016/0883-2927(89)90067-X

Pumure, I., J.J. Renton, and R.B. Smart. 2010. Ultrasonic extraction of arsenic and selenium from rocks associated with mountaintop removal/valley fills coal mining:estimation of bioaccessible concentrations. Chemosphere 78:1295–1300. doi:10.1016/j.chemosphere.2010.01.020

Rietra, R.P.J.J., T. Hiemstra, and W.H. van Riemsdijk. 2001. Comparison of selenate and sulfate adsorption on goethite. J. Colloid Interface Sci. 240:384–390. doi:10.1006/jcis.2001.7650

Su, C., and D.L. Suarez. 2001. Selenate and selenite sorption on iron oxides: An infrared and electrophoretic study. Soil Sci. Soc. Am. J. 64:101–111. doi:10.2136/sssaj2000.641101x

U.S. Environmental Protection Agency. 1987. Ambient water quality criteria for selenium. EPA/440/5-87/006. USEPA Office of Water, Regulations and Standards, Washington, DC.

Vesper, D.J., M. Roy, and C.J. Rhoads. 2008. Selenium distribution and mode of occurrence in the Kanawha formation, southern West Virginia, U.S.A. Int. J. Coal Geol. 73:237–249. doi:10.1016/j.coal.2007.06.003

Zhang, P., and D.L. Sparks. 1990. Kinetics of selenate and selenite adsorption/desorption at the goethite/water interface. Environ. Sci. Technol. 24:1848–1856. doi:10.1021/es00082a010

Ziemkiewicz, P.F., M. O'Neal, and R.J. Lovett. 2011. Selenium leaching kinetics and in-situ control. Mine Water Environ. 30:141–150. doi:10.1007/s10230-011-0154-4